Combined modeling and experimental approach for the development of dual-release polymer millirods

Feng Qian, Gerald M. Saidel, Damon M. Sutton, Agata Exner, Jinming Gao[*]

Cancer-Targeted Drug Delivery Laboratory, Department of Biomedical Engineering, Case Western Reserve University, 10900 Euclid Avenue, Cleveland, OH 44106, USA

Abstract

This paper describes a combined modeling and experimental approach for the design and development of a polymer device to provide local drug therapy to thermally ablated solid tumors. The polymer device, in the shape of cylindrical millirod, will be implanted via image-guided procedures into the center of the ablated tumor. Drug released from the millirod aims to eliminate residual cancer cells at the boundary of the normal and ablated tissue following thermal ablation to provide an effective treatment of the total tumor volume. The design of the millirod release kinetics is based on a mathematical model of drug transport in the ablated tumor and the surrounding normal tissue. The optimal release kinetics consists of a dual-release process—a burst release followed by sustained release—to provide the most optimal drug pharmacokinetics at the ablation boundary. Model analysis leads to a quantitative correlation of burst dose and release rates to the ablation size and the drug concentration at the ablation boundary. A three-layer polymer millirod is produced by a dip-coating method, and in vitro study demonstrates the dual-release kinetics in which a burst release occurs within 2 h followed by a sustained release over 7–10 days. Independent control of the burst and sustained release rates is achieved by varying the structural composition of the outer and middle layers of the millirods, respectively. Results from this study provide the rational basis and experimental feasibility of dual-release millirods for further efficacy studies in solid tumors.
© 2002 Elsevier Science B.V. All rights reserved.

1. Introduction

Targeted drug delivery was first conceptualized in the early 1900s by a German pharmacist, Paul Ehrlich, who coined the term 'magic bullet' to describe an ideally site-specific drug. Until recently, site-specific delivery of drugs has remained an elusive goal despite intensive research efforts in both academia and industry. In the last 20 years, traditional research efforts have been mostly focused on a 'chemical' targeting strategy, which relies on the molecular recognition of unique surface signatures of targeting tissues by chemical ligands (e.g., antibody–drug conjugates, immunoliposomes) [1,2]. Although initial successes have been achieved in cell culture experiments in vitro, these systems were not very

[*]Corresponding author. Tel.: +1-216-368-1083; fax: +1-216-368-4969.

E-mail address: jmg23@po.cwru.edu (J. Gao).

successful in vivo due to a number of factors, such as non-specific uptake by the reticuloendothelial systems, enzymatic degradation, decreased targeting capability under shear conditions, etc. [3–5]. In the case of solid tumors, this targeting approach is further thwarted by a hydrodynamic barrier due to the high interstitial pressure within the solid tumor [6]. These numerous physiological barriers strongly suggest that a simpler targeting method that can bypass these barriers should be explored.

At our institution, we are currently developing a 'physical' targeting strategy for tumor-targeted delivery of drugs. This approach aims to maximize the synergy between two dynamic fields of research—interventional radiology and controlled release drug delivery—to apply image-guided procedures to implant a drug delivery device directly into tumor tissues for controlled delivery of anticancer drugs. Our current research focuses on the development of a combination therapy consisting of image-guided radiofrequency (RF) ablation of solid tumors followed by intratumoral drug delivery [7,8]. In this paradigm, RF ablation destroys most of the tumor tissue by heat; after RF ablation, intratumoral drug delivery provides a sustained local chemotherapy to eliminate residual cancer cells and prevent tumor recurrence. This combination therapy has several potential advantages: (1) the procedure benefits from the pinpoint accuracy of a high-resolution image-guidance procedure [9–13] for minimally invasive and local tumor destruction; (2) RF ablation destroys the majority of tumor tissue and, consequently, reduces the drug dosage required for intratumoral delivery; (3) destruction of the tumor vasculature by RF ablation can reduce drug loss by perfusion and increase drug diffusion in ablated tissues (previous studies have shown that drug penetration reached 5.2 mm in ablated tissue versus 1.2 mm in non-ablated liver tissue [7]); (4) intratumoral delivery can improve delivery efficiency and reduce drug toxicity and morbidity that are usually associated with systemic chemotherapy.

Unlike systemic chemotherapy where drugs are delivered from 'outside-in' (i.e., drug molecules first enter the blood circulation and then distribute to the tumor tissue), intratumoral drug delivery provides an opposite 'inside-out' means of delivery. As a result, existing clinical pharmacokinetic models for systemic drug administration cannot be used to optimize the dosage regimens in the local drug therapy. In this study, we aim to establish a conceptual framework based on drug transport processes in vivo for the rational design of polymer devices for intratumoral drug delivery. To achieve the most optimal drug pharmacokinetics, model analysis proposes dual-release kinetics consisting of a burst release followed by a sustained release of drugs from the polymer millirods. Moreover, a quantitative correlation of burst dose and sustained release rates is obtained with the ablation size and the targeted drug concentration at the ablation boundary. This quantitative relationship provides the design criteria for the polymer millirods in drug delivery applications within ablated solid tumors. Experimentally, the dual-release millirods are produced by a dip-coating procedure with independent control of burst dose and sustained release rates to permit future validation of the millirod design.

2. Model basis for the rational design of dual-release millirods

2.1. Drug transport in ablated and normal tissues

First, we developed a mathematical model that describes the drug release and transport processes from the polymer millirod implanted at the center of the ablated tumor to the site of action. The targeted site of action is located at the boundary of the ablated and non-ablated tissue, where residual viable cancer cells are most likely present (Fig. 1). Within the ablated tissue where no viable cells or blood circulation exist, only diffusion occurs [7]. We begin with a mass transport model that describes the dynamics of drug concentration $C_a(r, t)$ in the ablated region ($r_p < r < r_s$) as a function of radial distance from the millirod:

$$\frac{\partial C_a}{\partial t} = \frac{D_a}{r} \frac{\partial [r \partial C_a / \partial r]}{\partial r}, \quad r_p < r < r_s \quad (1)$$

where D_a is the diffusivity within the ablated tissue. Since the length of the millirod is much greater than its diameter, we assume that the diffusion process occurs primarily in the radial direction. When the drug diffuses into the surrounding viable tissue, it will be taken up by cells or lost by perfusion. The governing equation for the drug concentration $C_n(r, t)$ in the non-ablated region ($r_s \leq r$) is
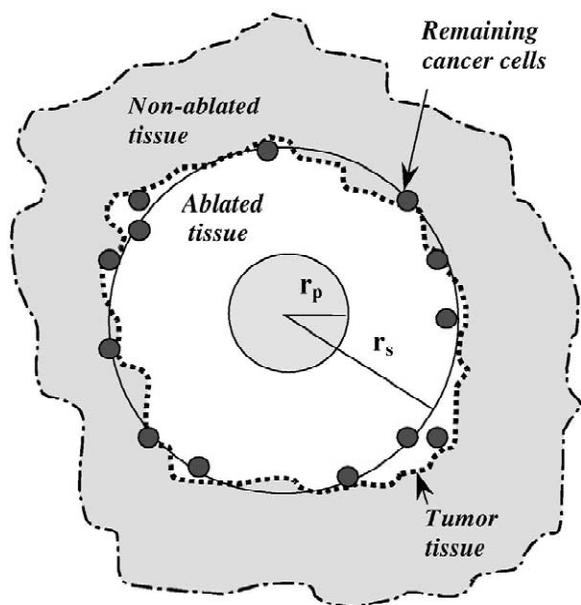
Fig. 1. Schematic representation of the implanted millirod inside the thermoablated tumor tissue. The radii of the millirod and the ablated area are denoted by r_p and r_s, respectively.

$$\frac{\partial C_n}{\partial t} = \frac{D_n}{r} \frac{\partial[r\partial C_n/\partial r]}{\partial r} - k_n C_n, \quad r_s < r \tag{2}$$

where D_n is the diffusivity within the non-ablated tissue and k_n is the combined rate coefficient of cell uptake and drug perfusion.

Because the time constant for sustained release is much greater than the other rate processes, we assume quasi-steady conditions in the solution to these equations. Correspondingly, the rod radius is considered as a quasi-steady because its time constant is expected to be much larger than that for the drug transport within the tissue. At steady state, the governing equation in the ablated region ($r_p < r < r_s$) is

$$r\frac{d^2 C_a}{dr^2} + \frac{dC_a}{dr} = 0 \tag{3}$$

The general solution for this equation is

$$C_a = b_1 \ln r + b_2 \tag{4}$$

where b_1 and b_2 are constants. At the interface between the polymer rod surface and ablated region, the release flux J equals the diffusion flux:

$$r = r_p: J = -D_a \frac{\partial C_a}{\partial r} \tag{5}$$

If we apply this condition and the definition of the drug concentration at the ablated tissue boundary $C_s = C_a(r_s)$, then the constants can be evaluated to yield

$$C_a = \frac{r_p}{D_a} J \cdot \ln\left(\frac{r_s}{r}\right) + C_s \tag{6}$$

At steady state, drug transport and uptake in the non-ablated region ($r_s < r$) is simplified to

$$\frac{d^2 C_n}{dr^2} + \frac{1}{r}\frac{dC_n}{dr} - \frac{k_n}{D_n}C_n = 0 \tag{7}$$

whose general solution is:

$$C_n = b_3 K_0(\beta r) + b_4 I_0(\beta r)$$

where $K_0(\beta r)$ and $I_0(\beta r)$ are modified Bessel functions of zero order and $\beta = \sqrt{k_n/D_n}$. The constants b_3 and b_4 can be evaluated from the boundary conditions. Since the drug concentration goes to zero with distance from the millirod source, we must set $b_4 = 0$. Noting that $C_n(r_s) = C_s$, we can write the solution as

$$C_n = C_s \frac{K_0(\beta r)}{K_0(\beta r_s)} \tag{8}$$

To evaluate C_s, we apply the condition of drug flux continuity between ablated and non-ablated regions:

$$r = r_s: D_a \frac{\partial C_a}{\partial r} = D_n \frac{\partial C_n}{\partial r} \tag{9}$$

Consequently, from Eqs. (6) and (8), we obtain

$$C_s = \frac{(r_p/r_s)(J/\beta D_n)K_0(\beta r_s)}{K_1(\beta r_s)} \tag{10}$$

where $K_1(\beta r)$ is the modified Bessel function of the first order. Knowing C_s, we can use Eqs. (6) and (8) to compute the steady-state concentration distribution in both regions.

2.2. Quantitative design of drug release

At the millirod surface, the drug release rate per unit length of millirod (R_D) is proportional to the drug flux:

$$R_D = 2\pi r_p J = 2\pi \beta D_n r_s C_s K_1(\beta r_s)/K_0(\beta r_s) \tag{11}$$

This relationship can be used in designing drug release kinetics to achieve a therapeutic concentration C_T at the ablation boundary, i.e., $C_s = C_T$. The maintenance dose A_M needed to keep $C_s = C_T$ at steady-state for a time period t_M is $A_M = t_M R_D$. Before this sustained effect is achieved at steady state, a burst dose A_B can be released so that C_T can be reached quickly for an early therapeutic effect. For an accurate estimate of A_B, the dynamic model equations must be solved with a specified time-varying release rate. As an approximation, we can obtain the minimal bound on A_B by integrating the steady-state concentration over both the ablated and non-ablated regions. This approximation neglects the effect of drug loss in the non-ablated region during the transient period:

$$A_B = \int_{r_p}^{r_s} 2\pi r \cdot C_a(r)\, dr + \int_{r_s}^{\infty} 2\pi r \cdot C_n(r)\, dr$$

$$= \frac{R_D}{4D_a}\left[2r_p^2 \ln\left(\frac{r_p}{r_s}\right) + r_s^2 - r_p^2\right]$$

$$+ \frac{C_T(r_s^2 - r_p^2)}{2r_p} + \frac{R_D}{D_n} \tag{12}$$

The minimum drug dosage needed per unit length of the millirod is therefore the sum of the burst and maintenance doses, $A = A_B + A_M$.

2.3. Model design for dual-release millirods

From the steady-state solution of the mathematical model, the drug distribution profiles were obtained in ablated and non-ablated regions (Fig. 2). The concentration distribution depends on the model parameters (r_p, r_s, D_a, D_n, k_n, J). In this simulation, we chose to use the D_n and K_n values for an anticancer drug, BCNU, in brain tissues as reported from Saltzman's lab ($D_n = 4.3 \times 10^{-7}$ cm^2 s^{-1}, $k_n = 4.4 \times 10^{-4}$ s^{-1}) [14,15]. In addition, we assume $D_a = D_n$. It should be noted that model design based on these parameters is intended only for demonstration of principle. Current work is in progress to determine these parameters in the normal and ablated liver tissues for doxorubicin.

Fig. 2 shows the effect of varying the release rate R_D on the simulated concentration distribution profiles, where faster release rates from the polymer millirods led to higher concentrations at the ablation
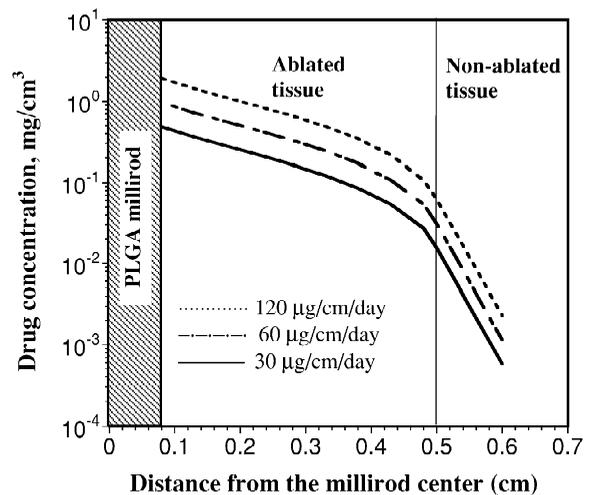

Fig. 2. Steady-state drug concentration distribution as predicted by the mathematical model. We assume that $r_p = 0.08$ cm, $r_s = 0.5$ cm. $D_n = D_a = 4.3 \times 10^{-7}$ cm^2 s^{-1}, $k_n = 4.4 \times 10^{-4}$ s^{-1}. The drug distribution profiles are modeled for three drug release rates ($R_D = 30$, 60, 120 μg/cm per day).

boundary. Fig. 3 illustrates the concept for rational design of polymer millirods. From the steady-state solution of the model, the values of A_B and R_D were plotted as a function of the targeted concentration C_T at the ablation boundary for three ablation sizes. For specific values of C_T and r_s, corresponding values of A_B and R_D can be obtained for the design of release kinetics of the polymer millirods. For example, to achieve $C_T = 10$ μg/cm^3 concentration at $r_s = 0.5$ cm, we need to develop millirods with $A_B = 2.2$ mg/cm and $R_D = 20$ μg/cm per day. The large value of A_B illustrates a clear advantage for introducing the burst dose in the millirod design.

3. Experimental methods

3.1. Materials

Poly(D,L-lactide) (PLA, inherent viscosity 0.67 dl/g) and poly(D,L-lactide-*co*-glycolide) (PLGA, lactide:glycolide = 1:1, MW 50 000 Da, inherent viscosity 0.65 dl/g) were purchased from Birmingham Polymers, (Birmingham, AL). Poly(ethylene glycol) (PEG, M_n 4600) and poly(ethylene oxide) (PEO, M_v 200 000) were obtained from Aldrich (Milwaukee, WI). Doxorubicin–HCl solution was
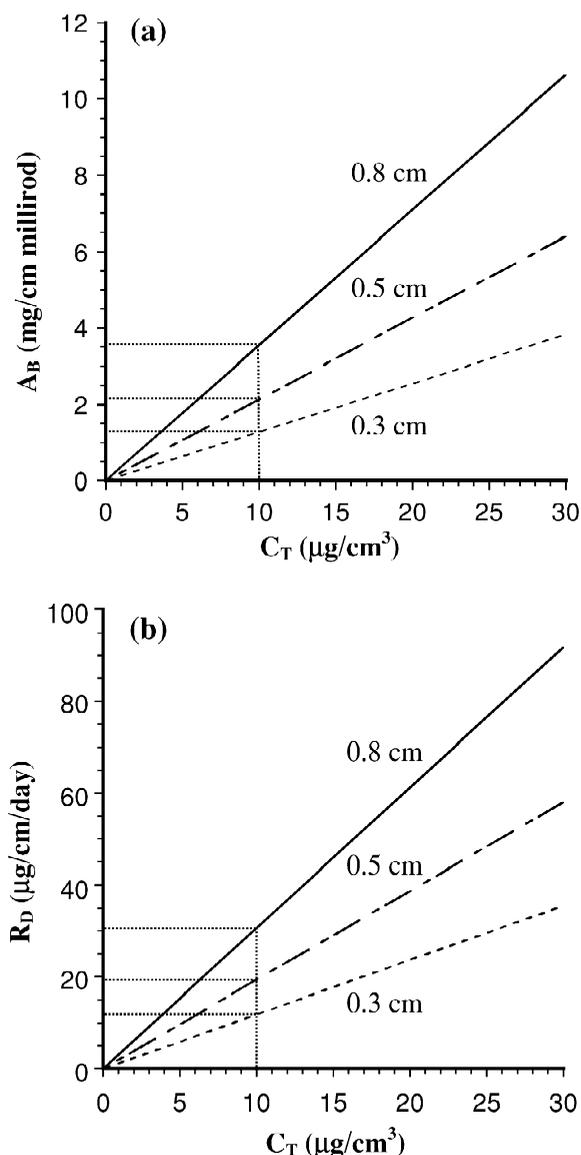
Fig. 3. Rational design of burst dose (A_B) and drug release rate (R_D) to reach and maintain a targeted drug concentration (C_T) at r_s. Three ablation sizes are evaluated at $r_s = 0.3$, 0.5 and 0.8 cm.

purchased from Bedford Laboratories (Bedford, OH).

3.2. Fabrication of doxorubicin-loaded, dual-release millirods

The doxorubicin–HCl solution was first desalted by dialysis in distilled water and then the purified doxorubicin solution was lyophilized to provide fine powder. PLGA microspheres (size: 5 μm) were produced by a single emulsion procedure [16]. Monolithic PLGA millirods containing 16% doxorubicin, 24% NaCl and 60% PLGA were fabricated by a compression-heat molding procedure [16]. Briefly, doxorubicin, NaCl and PLGA microspheres were weighed separately according to the final loading densities and the three components were placed in a plastic tube and physically mixed by vortex for 10 min. The mixture was placed into a Teflon tube (I.D. 1.6 mm) and then the Telfon tube was placed inside a stainless steel mold. The mold was put inside an iso-temp oven at 90 °C (Fisher Model 282A, set point accuracy <2 °C) for 2 h to allow the annealing of PLGA polymer. Compression pressure of 4.6 MPa was applied during the annealing process by a copper weight. After cooling down to room temperature, the millirods were pushed out of the Teflon tube by a stainless-steel plunger. The monolithic millirods have a diameter of 1.6 mm, and their length was cut to 10 mm.

Dual-release millirods were fabricated by applying two additional dip-coating procedures on the monolithic millirods. The PEG/PLA layer (middle layer) was formed by dipping the monolithic PLGA millirods into PEG/PLA solution in CH_2Cl_2. The total polymer concentration was 200 mg/ml and three different PEG in PLA percentages were used: 5, 10 and 20%. The dipping speed was controlled by a vertically placed syringe pump at 2 mm/s. After the control layer was completely dried, the burst layer was formed by dipping the millirod into doxorubicin/PEO suspension (100 mg/ml, 75% doxorubicin, 25% PEO in CH_2Cl_2). High-molecular weight PEO was used to increase the viscosity of the dipping solution. The number of dippings in doxorubicin/PEO suspension was used to control the burst dose. The dimension of the millirods is 10 mm in length, 1.8–2.0 mm in diameter depending on the thickness of the coated layers.

3.3. In vitro release studies

In vitro release studies were carried out in 25 mM Tris buffer (pH=7.4) at 37 °C. Each millirod was placed in a glass vial containing 2 ml Tris buffer. The sample vials were placed in an orbital shaker (C24 model, New Brunswick Scientific) with a

rotating speed of 100 rpm. At each time point, 2 ml of solution were removed for concentration measurement and 2 ml of fresh buffer were added. The concentration of released doxorubicin was measured by a UV–Vis spectrophotometer (Perkin-Elmer Lambda 20 model) at its maximum adsorption wavelength (480.8 nm). The extinction coefficient of doxorubicin at this wavelength is 16.8 ml/(cm·mg).

3.4. SEM analysis

Scanning electron microscopy (SEM, Jeol model 840) was used to study the morphology of the cross-section of the dual-release PLGA millirod. Freeze-fracturing in liquid nitrogen was used to provide a smooth and even millirod cross-section. Before SEM analysis, the sample was mounted on an aluminum stub by double-sided tape and sputter coated with Pd (10 nm thick). SEM analysis was carried out at an accelerating voltage of 20 kV.

4. Results

4.1. Structural composition of dual-release millirods

The dual-release polymer millirods consist of three structural components. The outer water-soluble doxorubicin/PEO layer provides the initial burst release of the drug after contact with biological fluid. After dissolution of the outer layer, the sustained release rate of doxorubicin is controlled by the middle PEG/PLA layer. The inner core of doxorubicin–PLGA matrix serves as the drug reservoir for sustained release. For this study, the inner monolithic PLGA millirods (16% doxorubicin) were kept the same for all the dual-release millirods. The PEG composition in the middle layer (5, 10, 20%) was

varied to control the sustained release rate. Higher PEG content produces higher porosity in the middle layer and, therefore, a faster drug permeation and release rate. The burst dose was controlled by the thickness of the outer PEO layer loaded with 75% doxorubicin. Table 1 lists five types of dual-release millirods with different structural compositions and release properties.

4.2. In vitro characterization of millirod release profiles

Fig. 4a shows the cumulative release of doxorubicin from three types of dual-release millirods with different burst doses (A_B), but similar sustained-release rates (R_D). These millirods shared the same inner core and rate-control (middle PEG/PLA) layer, but the thickness of the outer layer differed. All three types of millirods demonstrated the dual-release kinetics: a steep initial burst release phase due to the dissolution of the outer PEO layer followed by a sustained release phase controlled by the middle layer (10% PEG in PLA). Millirods B1S2, B2S2 and B3S2 have burst doses of 0.26, 0.65 and 1.48 mg/(cm millirod), respectively, within the first 2 h of release. For these millirods, the sustained dose (A_M, amount of doxorubicin contained inside the inner drug reservoir) was approximately 3.5 mg/(cm millirod), and the sustained release (constant slope) phase was maintained for about 7 days (or 170 h) at approximately 0.4 mg/(day·cm millirod).

Fig. 4b shows the cumulative release of doxorubicin from three types of dual-release millirods with the same burst dose, but different sustained release rates. These millirods shared the same inner core and burst dose layer (outer PEO layer), but the rate-control (middle PEG/PLA) layers differed. The PEG composition in the middle layer was set at 5, 10 and 20% for B3S1, B3S2 and B3S3 millirods, respective-

Table 1
Structural composition and release properties of different types of dual-release millirods

Millirod code	Inner core doxorubicin (%)	Middle layer PEG (%)	Dip-coating times of the outer layer	A_B (mg/cm)	R_D (mg/(day·cm))
B1S2	16	10	1	0.25	0.37
B2S2	16	10	2	0.65	0.39
B3S2	16	10	3	1.48	0.43
B3S1	16	5	3	1.55	0.27
B3S3	16	20	3	1.60	0.60

ly. The cumulative release profiles demonstrate similar burst dose at 1.55 mg/(cm millirod), but the sustained release rates increased with the increase of PEG composition. The average release rates were 0.27, 0.43 and 0.60 mg/(day·cm of millirod) for B3S1, B3S2 and B3S3 millirods, respectively. Since all the millirods shared the same sustained dose (A_M), the different release rates led to different time duration for the three types of dual-release millirods (Fig. 4b).

4.3. SEM study of millirod microstructure

To obtain mechanistic insight on the dual-release kinetics, we used SEM to analyze the microstructure of the doxorubicin millirods before and after the release experiments. Fig. 5a shows the SEM image of the cross-section of a representative B3S2 millirod before release. It clearly demonstrates the three-layer structure of the dual-release millirod: the outer doxorubicin/PEO layer, the middle PEG/PLA layer, and the inner monolithic millirod. The thickness of the outer and middle layers is approximately 150 and 80 μm, respectively. SEM analysis (Fig. 5b) of the same millirod composition after 7 days of drug release in Tris buffer (pH 7.4) shows that the outer PEO layer, which produces the initial burst, was completely dissolved. The PEG/PLA layer appeared to be porous, probably due to the leaching of water-soluble PEG molecules from the hydrophobic PLA matrix. The resulting membrane became the semi-permeable barrier that controls the rate of release from the inner drug reservoir. Finally, SEM shows the interconnecting pores and channels inside the polymer matrix of the inner core, which is consistent with the complete release of doxorubicin and NaCl (Fig. 4).

5. Discussion and conclusion

The delivery of a therapeutic agent to the site of action is the defining objective of any pharmaceutical treatment. The accessible concentration of the drug at the site of action and tissue exposure time are directly related to the pharmacological responses, whether therapeutic or toxic. In systemic chemo-therapy, drug plasma concentrations (ideally, drug
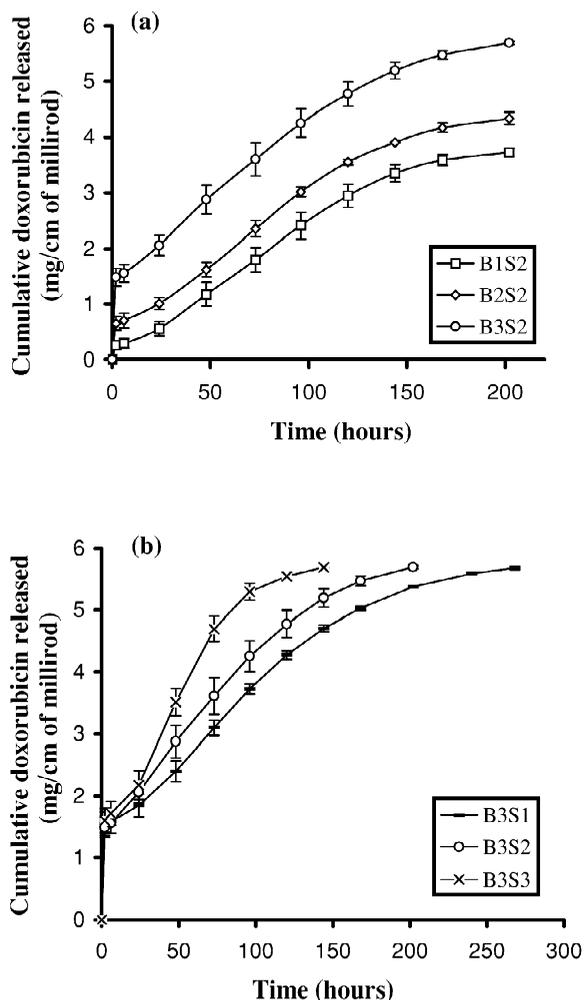

Fig. 4. Cumulative release profiles of dual-release millirods. The structural composition for each type of millirod is listed in Table 1. The error bars in Fig. 4 were measured from triplicate samples. (a) Millirods with the same sustained release rate, but different burst doses. (b) Millirods with the same burst dose, but different sustained release rates.

concentrations at the site of action should be used) are usually measured over time, and the area under the concentration–time curve (AUC) is calculated and related to pharmacological response. Typically, a desired steady-state concentration (C_{ss}) of the drug is chosen and a desirable range for the C_{ss} is defined as the therapeutic range [17]. Because most anticancer drugs have narrow therapeutic indices, their clinical applications require careful design of dosage reg-imens to achieve a fine balance between efficacy and
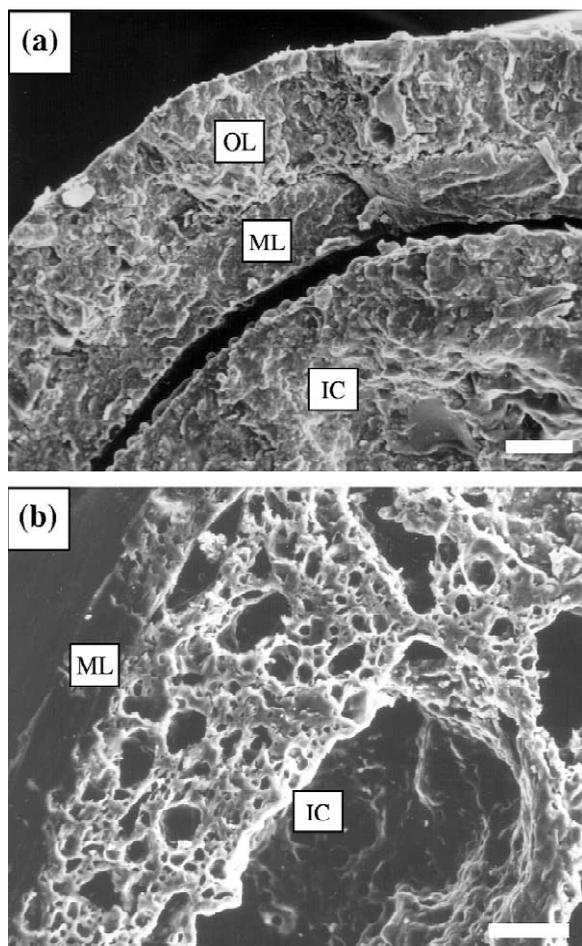
Fig. 5. SEM analysis of the dual-release millirods (B3S2) before release (a) and 7 days after release studies (b). OL, outer layer; ML, middle layer; IC, inner core. The scale bars in both images are 100 μm.
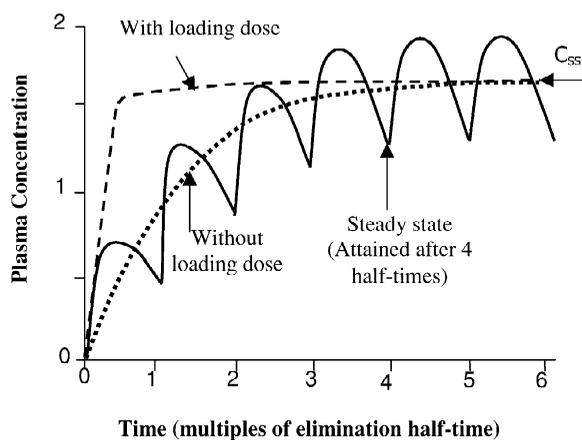

Fig. 6. Fundamental pharmacokinetic relationships for systemic administration of drugs. Dashed and dotted lines, continuous i.v. infusion; solid line, intermittent dosing. Partially adapted from Ref. [17].

toxicity. Fig. 6 illustrates the concentration–time curves for drugs either administered in a series of repeated doses or as a continuous infusion in systemic chemotherapy. The figure shows that continuous infusion of drugs permits a significantly less variable concentration range at C_{ss} than intermittent dosing. In addition, the use of a loading dose permits a much faster attaining of C_{ss} than the otherwise continuous dosing rate. The combined dosage administration and the resulting 'immediate and sustained' effect in systemic chemotherapy provide the conceptual basis for the design of polymer devices in our drug delivery applications.

The first step in a rational and quantitative design of polymer millirods that can deliver anticancer drug by an 'immediate and sustained' way requires the development of an appropriate mathematical model. For specific application in a thermally ablated liver tumor, we developed a dynamic model that describes the drug transport process in ablated and non-ablated regions. The objective of local drug therapy is to deliver drug at a sufficiently high concentration to the boundary of ablated tissue to kill the residual cancer cells. This requires that the therapeutic drug can be delivered to the targeted region quickly and the drug concentration can be maintained for a prolonged time. In this paper, we present a framework of procedures and working curves by which to calculate parameters required for fabrication of a polymer drug-delivery system.

Model simulations with a dual-release polymer millirod indicate how an initial burst dose followed by sustained release can provide optimal delivery of an anticancer drug to the ablation boundary. Without a burst dose, it would take a zero-order release device many days to reach the targeted region at the therapeutic concentration. Conceptually, the burst dose and the sustained release rate can be 'custom-designed' to meet the requirements to deliver therapeutic drug concentrations for differently sized tumors. Given the geometry of the tumor and ablated region, other model parameters such as drug dif-

fusivities and uptake in normal tissue must be estimated. More generally, the model must be validated by comparing simulated dynamic concentration distributions with those from experimental data. This requires knowledge of the time-varying release kinetics and numerical solution of the model equations.

Based on the current model simulations, we developed doxorubicin-containing polymer millirods with a controllable burst dose and sustained release rate. The three-layer design was partly derived from our previous design of membrane-encased, sustained release millirods [8]. Several factors can be used to adjust the membrane permeability and sustained release rate, such as the percentage of water-soluble components in the membrane, membrane thickness and tortuosity [8]. In the current study, PEG percentage in PLA provided effective controls over the release rates. The loading dose is introduced by an additional layer of doxorubicin/PEO, which can be easily controlled by the thickness of the layer and drug loading percentage. In vitro release studies (Fig. 4) demonstrated both the burst dose and the sustained release rate of the dual-release millirods are independently adjustable by design. This is essential for 'custom-designed' polymer millirods. In conclusion, the combined modeling and experimental approach provides a unique opportunity to develop dual release polymer millirods to achieve the maximal therapeutic effect in the local treatment of solid tumors.

Acknowledgements

References

[1] M. Willis, E. Forssen, Ligand-targeted liposomes, Adv. Drug Deliv. Rev. 29 (1998) 249–271.

[2] N. Hussain, Ligand-mediated tissue specific drug delivery, Adv. Drug Deliv. Rev. 43 (2000) 95–100.

[3] G. Gregoriadis, Engineering liposomes for drug delivery: progress and problems, Trends Biotechnol. 13 (1995) 527–537.

[4] S. Chandran, A. Roy, B. Mishra, Recent trends in drug delivery systems: liposomal drug delivery system—preparation and characterisation, Indian J. Exp. Biol. 35 (1997) 801–809.

[5] S. Weinbaum, S. Chien, Lipid transport aspects of atherogenesis, J. Biomech. Eng. 115 (1993) 602–610.

[6] R.K. Jain, Delivery of molecular and cellular medicine to solid tumors, Adv. Drug Deliv. Rev. 46 (2001) 149–168.

[7] J. Gao, F. Qian, A. Szymanski-Exner, N. Stowe, J. Haaga, In vivo drug distribution dynamics in thermoablated and normal rabbit livers from biodegradable polymers, J. Biomed. Mater. Res. 62 (2002) 308–314.

[8] F. Qian, N. Nasongkla, J. Gao, Membrane-encased polymer millirods for sustained release of 5-fluorouracil, J. Biomed. Mater. Res. 61 (2002) 203–211.

[9] D.H. Gronemeyer, S. Schirp, A. Gevargez, Image-guided radiofrequency ablation of spinal tumors: preliminary experience with an expandable array electrode, Cancer J. 8 (2002) 33–39.

[10] R. Heermann, B. Schwab, P.R. Issing, C. Haupt, C. Hempel, T. Lenarz, Image-guided surgery of the anterior skull base, Acta Otolaryngol. 121 (2001) 973–978.

[11] Y. Kono, S. Kanazawa, Y. Hiraki, CT-guided needle biopsy in malignant lymphoma: current techniques and its usefulness, Nippon Rinsho 58 (2000) 624–628.

[12] B.W. Long, Image-guided percutaneous needle biopsy: an overview, Radiol. Technol. 71 (2000) 335–359.

[13] T.M. Peters, Image-guided surgery: from X-rays to virtual reality, Comput. Methods Biomech. Biomed. Eng. 4 (2000) 27–57.

[14] L.K. Fung, M. Shin, B. Tyler, H. Brem, W.M. Saltzman, Chemotherapeutic drugs released from polymers: distribution of 1,3-bis(2-chloroethyl)-1-nitrosourea in the rat brain, Pharm. Res. 13 (1996) 671–682.

[15] J.F. Strasser, L.K. Fung, S. Eller, S.A. Grossman, W.M. Saltzman, Distribution of 1,3-bis(2-chloroethyl)-1-nitrosourea and tracers in the rabbit brain after interstitial delivery by biodegradable polymer implants, J. Pharmacol. Exp. Ther. 275 (1995) 1647–1655.

[16] F. Qian, A. Szymanski, J. Gao, Fabrication and characterization of controlled release poly(D,L-lactide-co-glycolide) millirods, J. Biomed. Mater. Res. 55 (2001) 512–522.

[17] L.Z. Benet, D.L. Kroetz, L.B. Sheiner, Pharmacokinetics, in: J.G.L.L. Hardman, P.B. Molinoff, R.W. Ruddon (Eds.), Goodman & Gilman's The Pharmacological Basis of Therapeutic, 9th Edition, McGraw-Hill Health Professions Division, New York, 1996, pp. 3–27.